DECEMBER 1982 LRP 216/82

MEASUREMENTS OF ELECTRON AND ION HEATING BY ALFVEN WAVES IN THE TCA TOKAMAK

A. DE CHAMBRIER, A. HEYM, F. HOFMANN, B. JOYE, R. KELLER, A. LIETTI, J.B. LISTER, P.D. MORGAN*, N.J. PEACOCK+, A. POCHELON, M.J. STAMP+

MEASUREMENTS OF ELECTRON AND ION HEATING BY ALFVEN WAVES IN THE TCA TOKAMAK

A. DE CHAMBRIER, A. HEYM, F. HOFMANN, B. JOYE, R. KELLER, A. LIETTI, J.B. LISTER, P.D. MORGAN*, N.J. PEACOCK+, A. POCHELON, M.J. STAMP+

Centre de Recherches en Physique des Plasmas
Association Euratom - Confédération Suisse
Ecole Polytechnique Fédérale de Lausanne
CH-1007 Lausanne / Switzerland

+ Culham Laboratory, Abingdon, England

* Present address: JET, Abingdon, England

ABSTRACT

Alfvén Wave Heating experiments have been carried out in the TCA Tokamak. Rf power up to 75 % of the value of the ohmic heating power has been delivered to the plasma. Increases in axial electron temperature of up to 80% ($\Delta T_e \sim 400eV$) and in axial ion temperature of up to 50% ($\Delta T_i \sim 75eV$) have been measured. The rf pulse is accompanied by an increase in the radiated power loss, which becomes peaked on axis, and which is due to line emission by impurities, dominantly iron.

1. INTRODUCTION

The experimental programme on the TCA Tokamak is devoted to the study of Shear Alfvén Waves. The first experiments carried out were antenna coupling measurements at low power to examine the magnitude of the loading and its dependance on the plasma parameters. This work has been already reported by BUGMANN et al. (1981) and DE CHAMBRIER et al. (1982 a, 1982 b, 1982 c). The main conclusions were that firstly, the general behaviour of the antenna system, itself described by DE CHAMBRIER et al. (1982 a), was remarkably close to that predicted by MHD calculations carried out by APPERT et al. (1982 a), and secondly, that a fine structure of enhanced loading peaks due to Discrete Alfvén Waves (DAW) exists. The DAW spectrum has subsequently been numerically studied by APPERT et al. (1982 b, 1982 c) and by MAHAJAN et al. (1982).

The background theoretical studies for Alfvén Wave Heating have been considerable, with major contributions having been made by TATARONIS and GROSSMAN (1973), HASEGAWA and CHEN (1974, 1975), KELLER et al. (1978), APPERT et al. (1980 a, 1980 b, 1982 d), BALET (1982), ELFIMOV (1980), PURI (1980), STIX (1981) and ROSS et al. (1981). Heating experiments have previously been carried out in stellarators by DEMIRKHANOV et al. (1976), DIKIJ et al. (1976), GOLOVATO et al. (1976) and OBIKI et al. (1977, 1978), and also in a theta-pinch by KELLER and POCHELON (1978). A useful review of experimental work is given by SHOHET (1978). At present, experiments are being carried out in four Tokamaks namely PRETEXT (Texas, USA), TORTUS (Sydney,

Australia), RO-5 (Sukhumi, USSR) with results reported by DEMIRKHANOV et al. (1982), and TCA from which results were reported by DE CHAMBRIER et al. (1982 d). The most impressive results to date had been obtained on the stellarator HELIOTRON-D in which both electron and ion heating were observed, but with $\Delta T_e < 100$ eV and $\Delta T_i < 20$ eV, with 400 kW of rf being delivered by a helical antenna structure operating at 405 kHz. The rf pulse lasted for only one millisecond however. This paper reports on results recently obtained on the TCA Tokamak with longer (30 msec) rf pulses and with rf power up to 130 kW being delivered to the plasma.

2. THE EXPERIMENT

The TCA Tokamak has been described in detail by CHEETHAM et al. (1980 a, 1980 b) and for the experiments described in this paper the operating characteristics can be summarized as :

$R, a = 0.61, 0.18$ m
$B\phi = 11.6$ and 15.1 kG
$q(a) = 6 - 3$
$I_p < 130$ kA
$n_e(0) = 2 - 4 \times 10^{19}$ m^{-3}

For all these experiments, the working gas was deuterium. The rf antenna structure is discrete with currents only in the poloidal plane. The antennae are constructed out of wide unshielded stainless steel plates in groups of three, above and below the plasma, with one set in each quadrant of the torus. By correctly phasing the antennae we dominantly excite different modes (n,m) defined by the Shear Alfvén Wave resonance condition, given, in cylindrical approximation, by

$$\omega^2 (r) = (n + m/q(r))^2 \frac{B\phi^2}{\mu_0 \rho(r) R^2} \qquad (1)$$

We denote the excitation structure by (N, M) and the waves excited by (n, m). Since the exciting structure is not pure, there is not a one to one correspondance between these definitions.

In this work we have only studied M = ± 1 excitation and the frequency remained fixed at 2.6 MHz. The rf power system itself has been described by DE CHAMBRIER et al (1982 e) and consists of an auto-oscillator connected to the eight antenna groups in parallel, by means of a tuned circuit for each group. The rf power delivered to the plasma is calculated from the measured values of the plasma loading resistance and the rf current, for each antenna circuit. Although the loading resistance can vary considerably during the pulse, due to the enhanced loading peaks corresponding to the excitation of a DAW, the power delivered does not vary too much, due to the internal impedance of the generator.

Early experiments were performed with N = 1,2 and 4 excitation and it was found that better results were obtained for N = 2, operating near the n = 2, m = + 1 continuum threshold close to which the n = 2, m = + 1 DAW is excited. Subsequently only experiments with an N = 2 excitation structure will be described in what follows. A detailed comparison between the different excitation structures will be carried out in the future.

A typical discharge is shown in Fig. 1. The toroidal field is 15.1 kG and the rf power ~ 70 kW. The dashed lines show the behaviour without the rf pulse and we make the following observations which generally hold for all discharges: there is an increase in line-integrated electron density which saturates during the rf pulse; there is an abrupt rise in the intensity of the Fe^{II} line emission (2599 Å), maintained throughout the pulse: the value of $\Lambda = \beta + li/2$ is also increased throughout the pulse: the line-averaged radiated power increases from the start of the rf pulse and saturates when the density increase saturates; there is an increase in the value of the apparent plasma resistance, $R_p + \dot{L}p/2$, calculated from the loop voltage and current waveforms, as a result of which there is a decrease in the plasma current during the rf pulse. We compensate for this latter effect by an increase in the applied loop volts. All the effects increase roughly linearly as a function of the delivered rf power. The behaviour of the electron and ion temperatures and the radiated power will be discussed in the following sections.

3. ELECTRON HEATING

Most of the results on electron heating were obtained at 15.1 kG, and all in deuterium. The typical behaviour of the electron temperature during the rf pulse is shown in Fig. 2. The full curve is the value of the electron temperature deduced from the intensity of soft X-rays passing through 150 μm and 300 μm Beryllium foils. The photons transmitted are in the range 1.5-4 keV, and the whole core of the plasma is observed. The value of the temperature obtained has been normalised before the rf pulse to agree with the Thomson Scattering measurements. These are shown in the figure as discrete points and a dashed line, and were obtained with a single-point two-pulse ruby laser which also allows us to check on the reproducibility of the electron temperature before the rf pulse is applied. Also shown are the rf power and antenna voltage waveforms. We see from the dip in the antenna volts that we cross a DAW resonance during the rf pulse. This is the $n = 2$, $m = +1$ DAW about whose resonance we performed all these experiments.

The electron temperature rises rapidly at the start of the rf pulse, saturates, and then drops. As the power is increased, the electron temperature rise increases linearly, as shown in Fig. 3, but the rate of decrease in temperature after the peak is also increased. At the maximum power delivered, 130 kW, the electron temperature fell quite rapidly and the plasma current also decreased fast. These two effects presently limit the delivered power. This value of rf power delivered is, however, a large fraction of the ohmic heating power

before the rf pulse. The increase in the plasma resistance at the end of the rf pulse is a sensitive function of the plasma resistance before the rf is applied, as shown in Fig. 4. From Fig. 3 and the line-averaged electron density of 2.5×10^{19} m^{-3} we calculate a heating factor $\bar{n}_e \Delta T_{eo}/P_{rf} = 7.7 \times 10^{19}$ eV/kWm^3. Although this remains the most oft-quoted figure of merit for a heating experiment, the true significance of the value obtained will only become apparent when detailed electron temperature and electron density profiles have been measured.

We take the change in the slope of $T_{eo}(t)$, as measured by the soft X-rays, and calculate $d/dt \int 3/2\ n_e\ T_e\ dV$ assuming a parobolic profile for the electron density and a parabola to the power 3 for the electron temperature. We obtain 55 kW to the electrons with a total rf power of 70 kW being delivered to the plasma.

4. RADIATED POWER LOSS AND SPECTROSCOPIC STUDIES

As already mentioned, there is a large observed increase in the total radiated power, associated with the rf pulse. The projected radiated power profile is measured by a scannable total radiation bolometer, during a series of shots, from which the radial profile is calculated by Abel inversion, assuming circular symmetry. The detector views the plasma from the side, well away from the limiter, and consists of a germanium resistance bolometer. A typical radial profile of the radiated power is shown in Fig. 5 (a) as a function of

time. The volume integrated radiated power, assuming no toroidal variation, is also shown in Fig. 5 (b) as a function of time during the rf pulse.

From these results we can make several observations. Firstly the increase is large and the total radiated power roughly equals the initial ohmic power input, 140 kW for the shot shown. The radiated power on axis 1.2 W/cm^3 almost reaches the local ohmic heating power of 1.5 W/cm^3 calculated from the assumed current profiles. The peakedness of the radial profile is such that it cannot be explained by a constant impurity concentration. Such a radiated power profile must be dominated by partly-stripped heavy impurities, since the light impurities only radiate significantly at the edge of the plasma. However the profile obtained in Fig. 6, assuming only iron as an impurity and the ionization state equilibria given by POST et al. (1977), is not as peaked as the profile in Fig. 5(a). A peaking of $n_{Fe}/n_e \sim(1-r^2/a^2)^4$ is required to simulate our observed results and this implies a strong enhancement of heavy impurities on axis during the rf pulse. If we again assume that iron is the only radiating impurity, the absolute value of the radiated power gives us an averaged impurity concentration of 1%, assuming the same equilibria model.

A Normal Incidence VUV spectrometer was used to monitor spectral emission in both photographic and photoelectric operation (STAMP et al., 1982). The spectrographic plates show clearly that although the density of most impurities increases during the rf pulse, the increase

in iron is dominant. Using photoelectric detection we have shown that the intensity of FeXVIII closely follows the radiated power signal, as seen in Fig. 7, and we attribute the major part of the radiated power increase to this ion and to the neighbouring ionization states. FeXIX is the most highly stripped iron ion observed in the VUV spectrum under our conditions.

Measurements of the Doppler widths of the core impurity ions were sufficiently accurate to give a measurement of the ion temperature in discharges with no additional heating. We found $T_i \sim 140eV \pm 50eV$ for NeIX added as a trace impurity. In these conditions the deuterium ion temperature, as measured by the Neutral Particle Analyser, was $\sim$ 200 eV. The agreement is close although in principle there is no requirement that the impurity ion be in perfect equilibrium with the main species.

In Fig. 8 we show the various ionization stages of oxygen up to OVII. We note that the behaviour of the peripheral ions OII to OVI is different from that of OVII which penetrates into the core. The more highly stripped iron ions FeXVI and FeXVIII also shown in Fig. 8, illustrate a similar behaviour to that of OVII. We do not attribute the step behaviour of the peripheral lines to a sudden change in impurity influx. Rather we consider that it is due to their extreme sensitivity to the edge profiles of both electron temperature and density. This is further indicated by the step-like change in the DC floating potential of the antennae during the rf pulse, shown in Fig. 9.

A more detailed calculation to estimate the concentration of iron was also performed on the basis of these spectroscopic data: using the known rate coefficients of the oxygen and iron lines we can calculate their relative concentrations. If we estimate that Zeff is dominated by oxygen, a concentration of 4 % is obtained for a value of Zeff = 3. This then leads to a concentration of $\sim$ 1% for iron, in agreement with the bolometric measurements. This method is outlined in more detail by STAMP et al. (1982).

5. ION HEATING

Experiments carried out at 11.6 kG in deuterium plasmas showed bulk heating of the ion population, with no evidence so far of the production of a high energy tail in the spectrum. The measurements were carried out using a multi-channel Neutral Particle Analyser, of the type described by AFROSIMOV et al. (1975), which views the plasma radially. Fig. 10 shows typical results when the rf pulse is applied. The conditions are such that the n = 2, m = + 1 DAW is crossed during the rf pulse, corresponding to a line-averaged density of 1.5 $\times 10^{19} m^{-3}$. As the rf power delivered to the plasma is increased, the value of ΔT_i increases linearly as shown in Fig. 11. The heating quality factor deduced from the figure is $\bar{n}_e \Delta T_{io}/Prf = 1.5 \times 10^{19}$ eV/kWm^3. From the change in the slope of the curve of ion temperature as a function of time we calculate an incremental increase of 5.5 kW to the ions, in a discharge with 70 kW of rf power delivered to the plasma. We assume that the ion temperature and density are parabolic.

The first measurements of ion temperature increase. reported by BUGMANN et al. (1981), were carried out at lower power in conditions in which a sizable fraction of the increase could be attributed to an increasing density and thus an increasing collisional electron-ion power transfer (Pei). If we consider this power transfer to be classical and the ion energy loss to be dominated by neoclassical diffusion we obtain the Artsimovich dependence of ion temperature, namely $T_i \sim (n_e B_\phi B_\theta)^{1/3}$. The observed 50% increase in ion temperature could only result from a 330% increase in density on this basis. The fact that the current decreases during the density rise makes this explanation even more unlikely. Assuming ion losses to be purely charge-exchange dominated does not alter this conclusion. Within reasonable limits modifications of the electron density and temperature radial profiles, to be subsequently verified, cannot fully explain the observed ion temperature increase either. A further possibility is that we are observing ion heating via the impurity ions which might extract energy from the wave directly. The fundamental resonances $\omega = \omega_{ci}$ exist in the plasma for some ionization states, but are mainly at the edge. One consequence of this model is that there would be a delay in the rise in the ion temperature, which would tend to increase parabolically at the beginning of the rf pulse. We see no evidence of this and have no reason to support this hypothesis. In fact we consider that at the end of the rf pulse the impurity ions are a power drain from the main ion species. We therefore claim to be measuring a direct input of rf power to the ions, provided the electron-ion transfer has remained classical during the rf pulse.

At 15.1 kG we observe less significant ion heating in terms of $\Delta T_i/T_i$. This can be explained by the fact that, from Equation (1), we must increase the electron density by a factor of $(15.1/11.6)^2$ to maintain the same Alfvén Wave structure at the same frequency. The electron-ion collisional power transfer increases by a factor of 2.5, assuming Artsimovich's scaling for ion temperature, and can conceal the additional rf power to a large extent. The increase in ion temperature should, on the basis of this argument, scale as B_ϕ^{-2} and in Fig. 12 we show ΔT_i as a function of B_ϕ, for two rf power levels, together with the predictable dependence on B_ϕ. We see that the agreement is not unreasonable.

6. POWER BALANCE

A preliminary attempt has been made to establish a power balance for one experimental condition, namely B_ϕ = 11.6 kG, I_p = 70 kA, deuterium, f = 2.6 MHz, excitation N = 2, M = 1. Fig. 13(a) shows the stored energy and power flows for this condition, integrated to r = 14 cm, for which parabolic ion temperature and density profiles and a parabola-cubed electron temperature profile have been assumed. The electron and ion diffusion losses are deduced via the calculated electron-ion collision power transfer, assumed to be classical. Fig. 13(b) shows the balance 15 msec after the beginning of the rf pulse, at which time the radiated power loss is close to its maximum, and the electron temperature has dropped below its peak value. To calculate the rf input power for each species, we must make an assumption

concerning the change in the power losses. We assume firstly that the electron confinement scales as density, i.e. that the electron power loss is independent of density, which is a frequently observed scaling at low powers and is in fact pessimistic for the calculation of rf efficiency. Secondly, the ion losses are assumed to scale as neoclassical plateau-diffusion losses. With these starting points we can calculate the power delivered to the electrons and ions, still assuming a classical value of P_{ei}. We obtain for the discharge under consideration an input of 53 kW to the electrons and 11 kW to the ions, to be compared with a total of about 70 kW delivered by the antennae. It would therefore appear that the efficiency of the core heating should be reasonable, provided that there are no gross changes in the radial profiles.

7. DISCUSSION

In the experiment described we have so far succeeded in delivering a maximum rf power of 130 kW to the plasma. The measurements show an increase in electron and ion temperature accompanied by an increase in electron density. The fact that the increase in the ion temperature cannot reasonably be attributed to the density increase is demonstrated at 11.6 kG. The treatment of the energy dissipation given by HASEGAWA and CHEN (1975) suggests that for a plasma of our low classical collisionality a negligible part of the wave energy should serve to heat the ions directly. The plasma viscosity would have to be extremely anomalous to explain our observed

ion temperature increase. OBIKI et al. (1977) also observed ion heating however. The neoclassical correction to classical viscosity may nonetheless be sufficient to explain the ion heating as proposed by VACLAVIK (1982); this is in principle testable due to the strong q-dependence predicted. It has been proposed by HASEGAWA (1982) that drift-wave turbulence at the plasma centre might also be a contributing factor. There is a large increase in radiated power due to impurities, mainly iron. Finally the preliminary power balance performed on these data suggests a reasonable efficiency of power absorption.

ACKNOWLEDGEMENTS

We wish to thank the TCA support team for their invaluable assistance in the experimental programme, and Culham Laboratory for the loan of a spectrometer and personnel. The bolometric measurements are the result of developmental work carried out by the University of Fribourg. This work was partly funded by the Swiss National Science Foundation.

REFERENCES

AFROSIMOV V.V., BEREZOSKII E.L., GLADKOVSKII I.P., KISLYAKOV A.I., PETROV M.P. and SADOVNIKOV V.A. (1975) Sov. Phys. Tech. Phys., 20, 1.

APPERT K., BALET B., GRUBER R., TROYON F. and VACLAVIK J. (1980 a) 8th Int. Conf. on Plasma Physics and Contr. Nucl. Fusion Research, Brussels, Vol. II, 43.

APPERT K., BALET B., GRUBER R., TROYON F., TSUNEMATSU T. and VACLAVIK J. (1980 b) 2nd Joint Grenoble-Varenna Int. Symp. on Heating in Toroidal Plasmas, Como, Vol. II, 643.

APPERT K., BALET B. and VACLAVIK J. (1982 a) Phys. Lett. 87A, 233.

APPERT K., BALET B., GRUBER R., TROYON F., TSUNEMATSU T. and VACLAVIK J. (1982 b) Plasma Physics 24, 8, 1147.

APPERT K., GRUBER R., TROYON F. and VACLAVIK J. (1982b) Procedings of the 3rd Joint Varenna-Grenoble International Symposium, EUR7979EN, Vol. 1, pp 203-212.

APPERT K., BALET B and VACLAVIK J. (1982 d) Nucl. Fusion 22, 903.

BALET B., APPERT K. and VACLAVIK J. (1982) Plasma Physics 24, 1005.

BUGMANN G., DE CHAMBRIER A., CHEETHAM A.D., HEYM A., HOFMANN F., JOYE B., KELLER R., LIETTI A., LISTER J.B., POCHELON A., SIMIK A., SIMM W., TONINATO J.L. and TUSZEL A. (1981) 10th European Conf. on Controlled Fusion and Plasma Physics, Moscow.

CHEETHAM A.D., HEYM A., HOFMANN F., HRUSKA K., KELLER R., LIETTI A., LISTER J.B., POCHELON A., RIPPER H., SCHREIBER R. and SIMIK A. (1980 a) Lausanne Report LRP 162/80

CHEETHAM A.D., HEYM A., HOFMANN F., HRUSKA K., KELLER R., LIETTI A., LISTER J.B., POCHELON A., RIPPER H., SIMIK A. and TUSZEL A. (1980 b) 11th Symp. on Fusion Technology, Oxford, Vol. 1, 601.

DE CHAMBRIER A., CHEETHAM A.D., HEYM A., HOFMANN F., JOYE B., KELLER R., LIETTI A., LISTER J.B., POCHELON A., SIMM W., TONINATO J.L. and TUSZEL A. (1982 a) Proceedings of the 3rd Joint Varenna-Grenoble International Symposium Vol. I, 161 EUR7979EN.

DE CHAMBRIER A., CHEETHAM A.D., HEYM A., HOFMANN F., JOYE B., KELLER R., LIETTI A., LISTER J.B., POCHELON A., SIMM W., TONINATO J.L. and TUSZEL A. (1982 b) Proceedings of the 3rd Joint Varenna-Grenoble International Symposium Vol III, 117 EUR7979EN.

DE CHAMBRIER A., CHEETHAM A.D., HEYM A., HOFMANN F., JOYE B., KELLER R., LIETTI A., LISTER J.B. and POCHELON A. (1982 c) Plasma Physics 24, 8, 893.

DE CHAMBRIER A., HEYM A., CHEETHAM A.D., HOFMANN F., JOYE B., KELLER R., LIETTI A., LISTER J.B., POCHELON A., SIMM W., TONINATO J.L. and TUSZEL A. (1982 d) Paper presented to the 9th Conference on Plasma Physics and Controlled Nuclear Fusion, Baltimore, USA.

DE CHAMBRIER A., HEYM A., HOFMANN F., JOYE B., KELLER R., LIETTI A., LISTER J.B., POCHELON A., SIMM W., TONINATO J.L. and TUSZEL A. (1982 e) Paper presented to the 12th Symp. on Fusion Technology, JÜlich.

DEMIRKHANOV R.A., KIROV A.G., LOZOVSKIJ S.N., NEKRASOV F.M., ELFIMOV A.G., IL'INSKIJ S.E. and ONISHCHENKO V.V. (1976) 6th Int. Conf. on Plasma Physics and Contr. Fusion Research, Berchtesgarden, Vol. III, 31.

DIKIJ A.G., KALINICHENKO S.S., KUSNETSOV Y.K., KURILKO P.I., LYSOJVAN A.I., PASHNEV V.K., TARASENKO V.F., SUPRUNENKO V.A., TOLOK V.T. and SHVETS O.M. (1976) 6th Int. Conf. on Plasma Physics and Contr. Fusion Research, Berchtesgaden, Vol. II, 129.

ELFIMOV A.G. (1980) 2nd Joint Grenoble-Varenna Int. Symp. on Heating in Toroidal Plasma, Como, Vol. II, 683.

GOLOVATO S.N., SHOHET J.L. and TATARONIS J.A. (1976) Phys. Rev. Lett. 39, 1272.

HASEGAWA A. and CHEN L. (1974) Phys. Rev. Lett. 32, 454.

HASEGAWA A. and CHEN L. (1975) Phys. Rev. Lett. 35, 370.

HASEGAWA A. (1982) private communication.

KELLER R., GRUBER R. and TROYON F. (1978) Joint Varenna-Grenoble Int. Symp. on Heating in Toroidal Plasmas, Grenoble, Vol. 2, 195.

KELLER R. and POCHELON A. (1978) Nucl. Fusion 18, 1051.

MAHAJAN S.M., ROSS D.W. and CHEN G.L. (1982) University of Texas Report FRCR 249.

OBIKI T., MUTOH T., ADACHI S., SASAKI A., IIYOSHI A. and UO K. (1977) Phys. Rev. Lett. 39, 812.

OBIKI T., MUTOH T., KINOSHITA S., SATO M., IIYOSHI A. and UO K. (1978) Joint Varenna-Grenoble Int. Symp. on Heating in Toroidal Plasmas, Grenoble, Vol. 1, 109.

POST D.E., JENSEN R.V., TARTER C.B., GRASBERGER W.H. and LOKKE W.A. (1977) Atomic Data and Nuclear Data Tables 20, 5, 397.

PURI S. (1980) 2nd Joint Grenoble-Varenna Int. Symp. on Heating in Toroidal Plasma, Como.

ROSS D.W., CHEN G.L. and MAHAJAN S.M. (1981) Fourth Topical Conf. on RF Heating in Plasma, Austin, Texas, paper B 14.

SHOHET J.L. (1978) Comments Plasma Phys. Cont. Fusion, 4, 37

STAMP M.J., POCHELON A., PEACOCK N.J., LISTER J.B., JOYE B. and GORDON H. (1982) Lausanne Report LRP 220/83.

STIX Th. H. (1981) 2nd Joint Grenoble-Varenna Int. Symp. on Heating in Toroidal Plasmas, Como, paper 6.

TATARONIS J.A. and GROSSMANN W. (1973) Z.Physik, 261, 203 and 217.

VACLAVIK J. (1982) private communication.

FIGURE CAPTIONS

Fig. 1 Plasma behaviour during the application of the rf pulse. (The dotted lines represent the plasma with no additional heating).

Fig. 2 Development of the electron temperature during the rf pulse. The solid line represents the soft X-ray measurements and the dashed line and points the Thomson scattering measurements. The antenna voltage is also shown.

Fig. 3 Dependence of the increase in electron temperature on the delivered rf power.

Fig. 4 Change in the plasma resistance at the end of the 30 msec rf pulse, as a function of the plasma resistance before the rf pulse.

Fig. 5 a) Development of the radial profile of radiated power during the rf pulse, and b) the total radiated power.

Fig. 6 Radiated power profile for a) constant and b) peaked concentration of iron, modelled from estimated profiles. Dotted lines show the effect of an additional 3 % Oxygen.

Fig. 7 Time dependence of the line-integrated emission of a) radiated power and b) FeXVIII line emission (947.7 Å).

Fig. 8 Time dependence of impurity lines during the rf pulse. a) Oxygen, b) Iron.

Fig. 9 Change in DC potential of the rf antennae during the rf pulse.

Fig. 10 Evolution of a) the ion distribution function and b) the ion temperature together with the calculated product $n_i n_o$. (11.6 kG, D_2, $q \sim 4.5$).

Fig. 11 Dependence of the ion temperature increase on the value of the delivered rf power.

Fig. 12 Dependence of the ion temperature increase on the toroidal field strength. The lines correspond to $\Delta T_i \sim B_\phi^{-2}$.

Fig. 13 Preliminary power balance a) without rf and b) with rf. (11.6 kG, 70 kA, N = 2, M = 1).

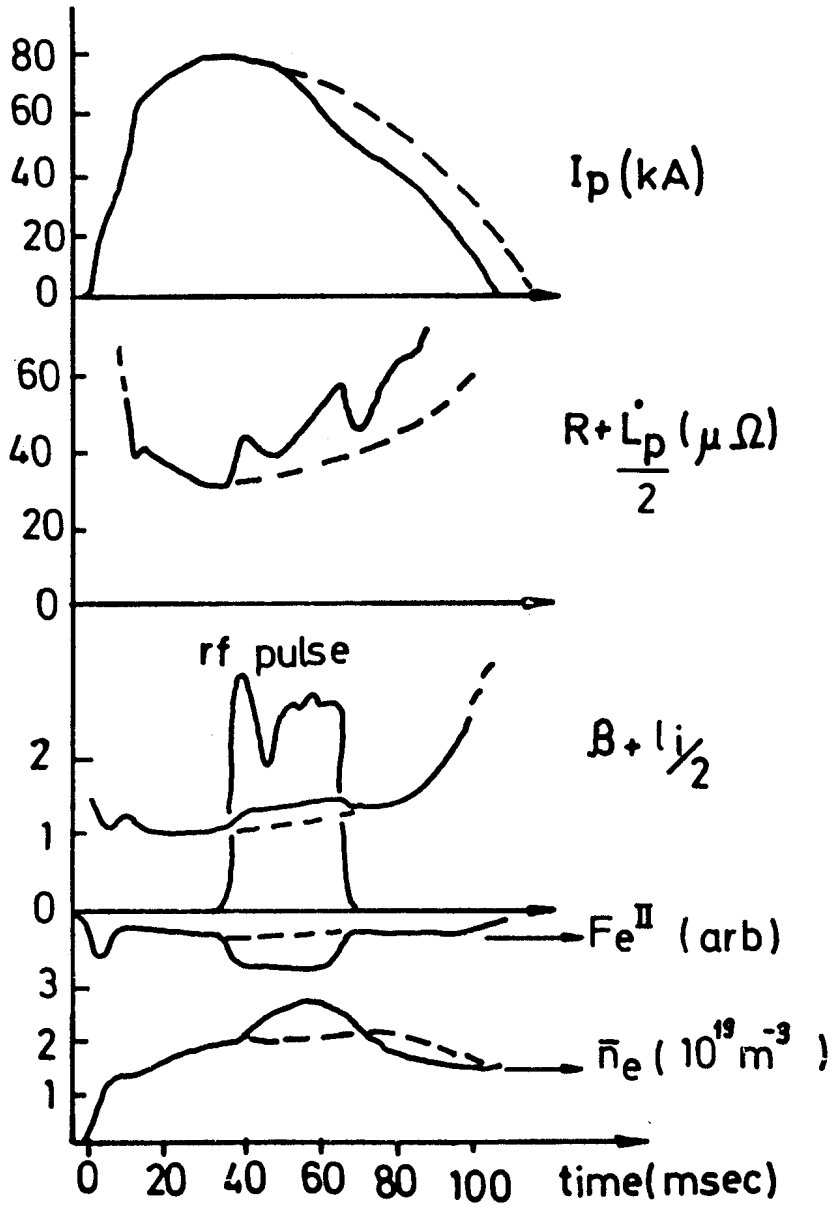
80
60
40
20
0
I_p (kA)
60
40
20
0
$R+\frac{\dot{L}_p}{2}$ ($\mu\Omega$)
rf pulse
2
1
0
$\beta + l_i/2$
Fe^{II} (arb)
3
2
1
$\bar{n}_e$ ($10^{19} m^{-3}$)
0 20 40 60 80 100 time(msec)

Fig.1

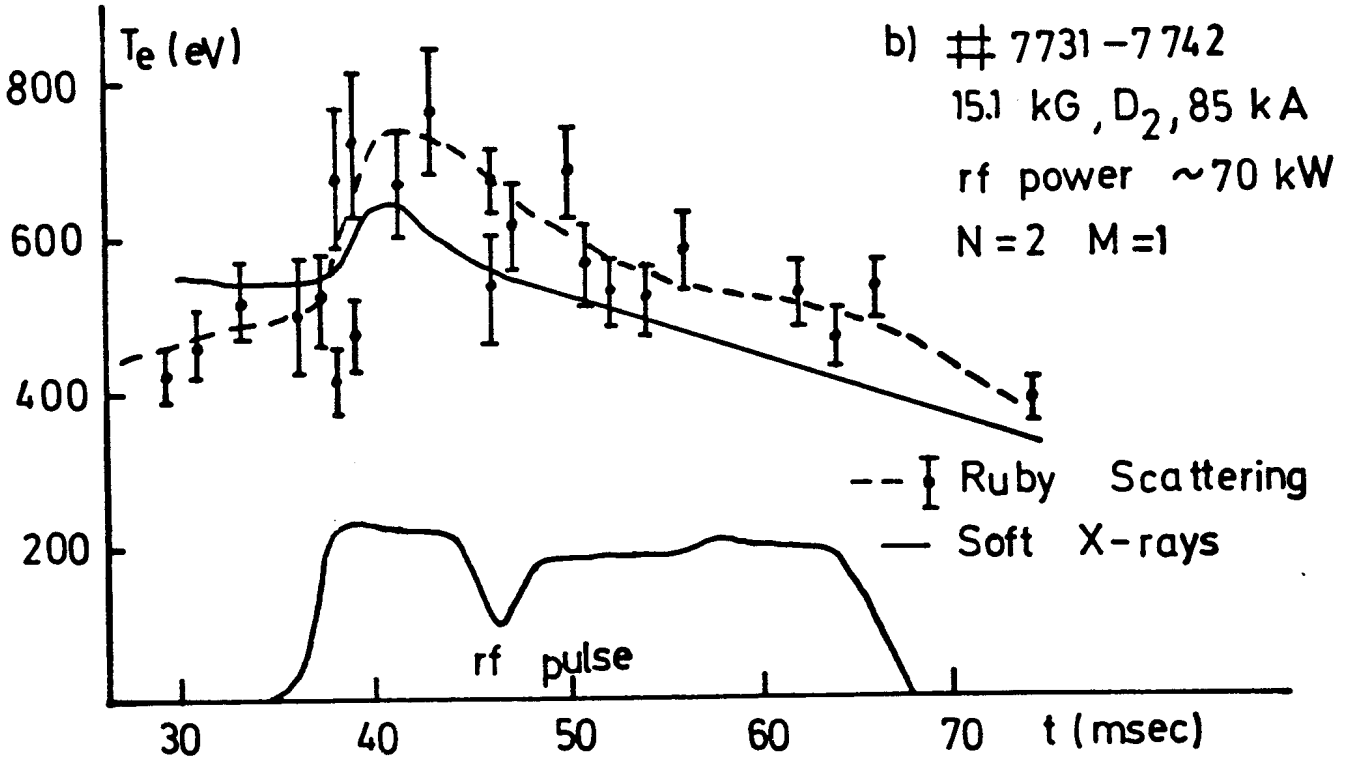
T_e (eV)
800
600
400
200
b) # 7731 – 7742
15.1 kG, D_2, 85 kA
rf power ~70 kW
N = 2 M = 1
Ruby Scattering
Soft X-rays
rf pulse
30
40
50
60
70
t (msec)

Fig. 2

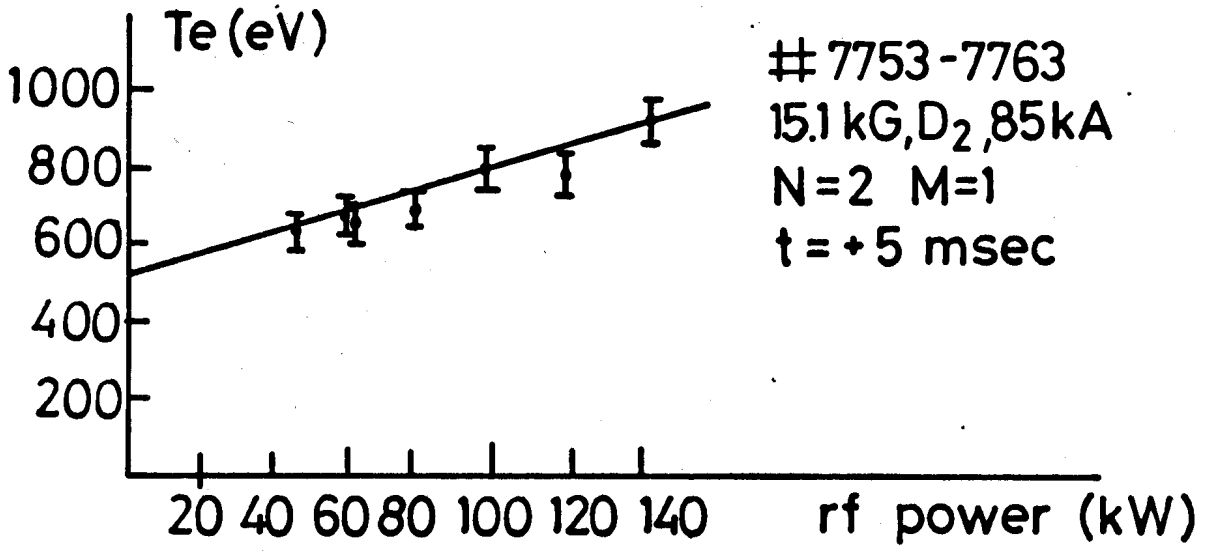
Te (eV)
1000
800
600
400
200
20 40 60 80 100 120 140
rf power (kW)
7753 - 7763
15.1 kG, D_2, 85kA
N = 2 M = 1
t = + 5 msec

Fig. 3

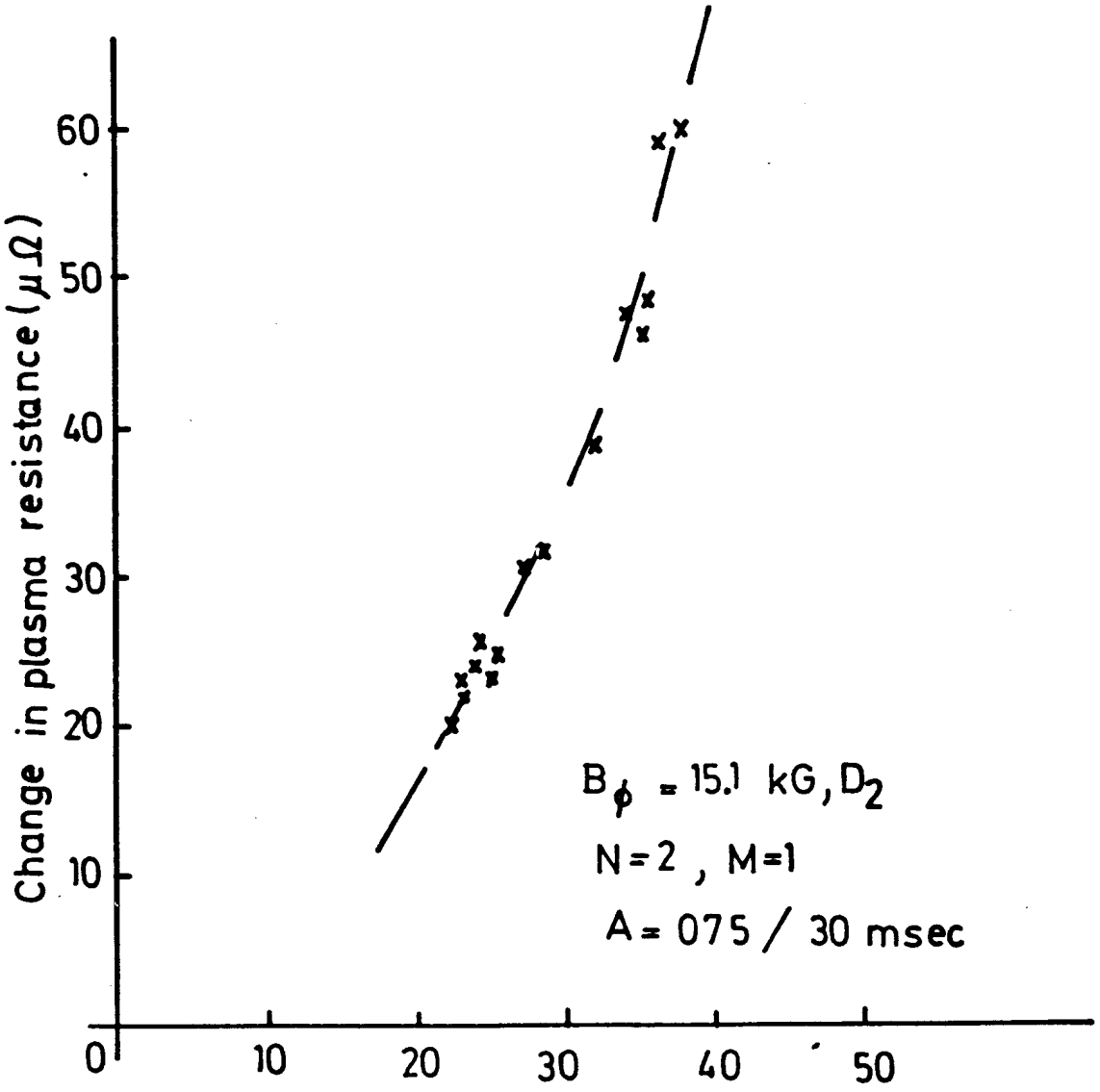
Change in plasma resistance (μΩ)
60
50
40
30
20
10
0
10
20
30
40
50
B_ϕ = 15.1 kG, D_2
N = 2 , M = 1
A = 075 / 30 msec
Plasma resistance before rf (μΩ)

Fig. 4

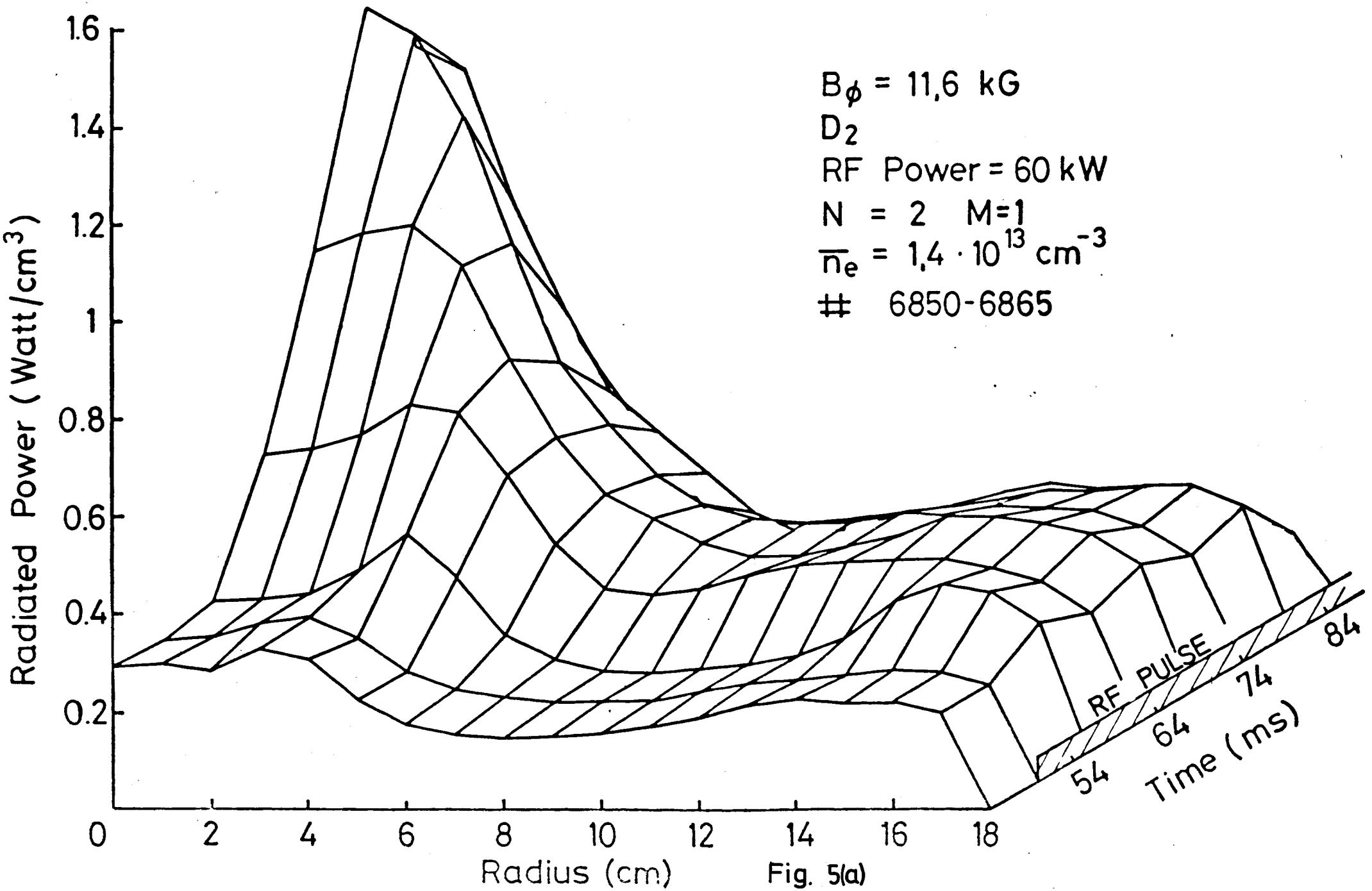
Radiated Power (Watt/cm^3)
1.6
1.4
1.2
1
0.8
0.6
0.4
0.2
0
2
4
6
8
10
12
14
16
18
Radius (cm)
B_ϕ = 11,6 kG
D_2
RF Power = 60 kW
N = 2 M=1
$\overline{n}_e = 1{,}4 \cdot 10^{13}$ cm^{-3}
6850-6865
RF PULSE
54
64
74
84
Time (ms)

Fig. 5(a)

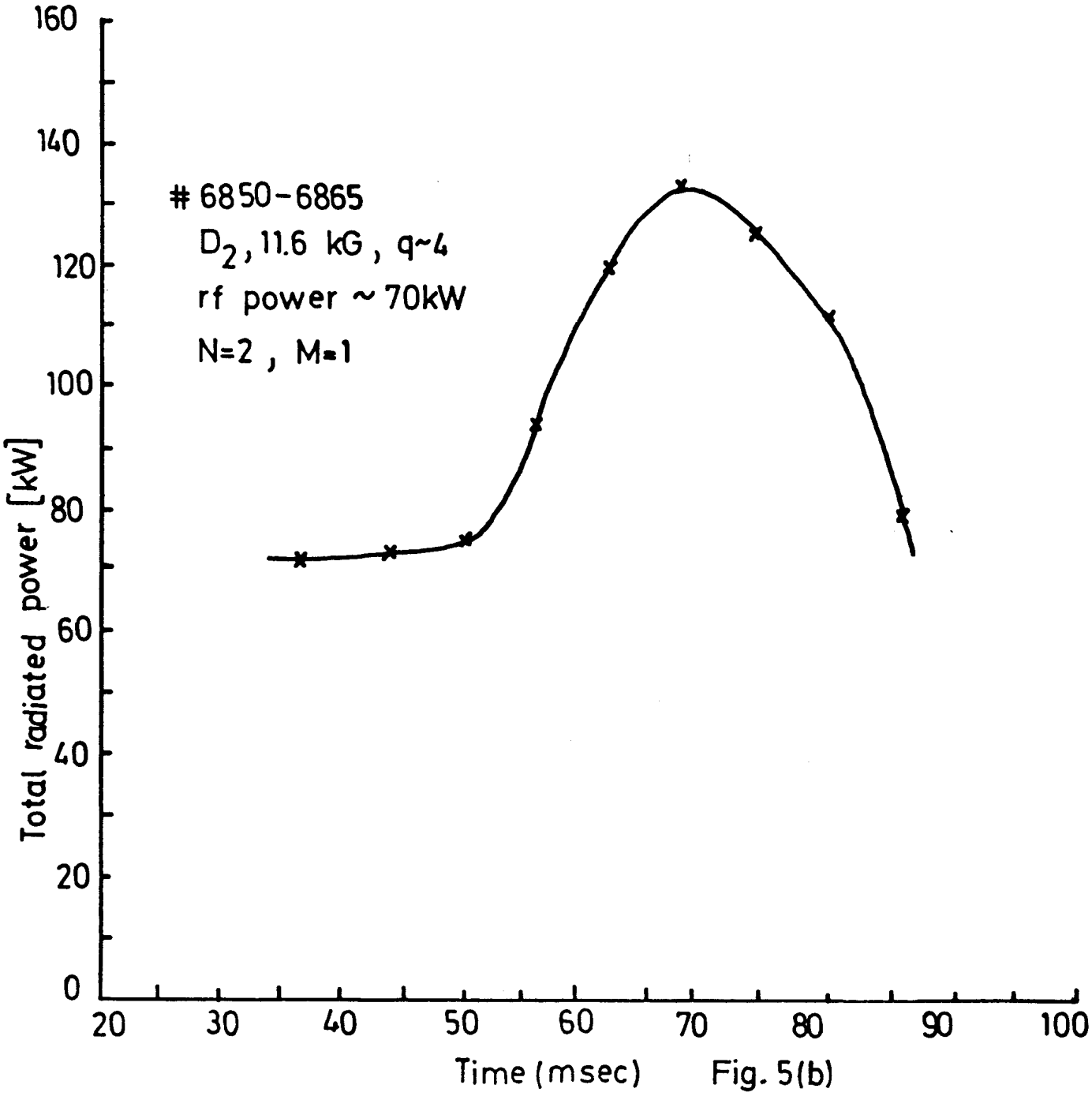
160
140
120
100
80
60
40
20
0
6850-6865
D_2, 11.6 kG, q~4
rf power ~ 70kW
N=2, M=1
Total radiated power [kW]
20
30
40
50
60
70
80
90
100
Time (msec)

Fig. 5(b)

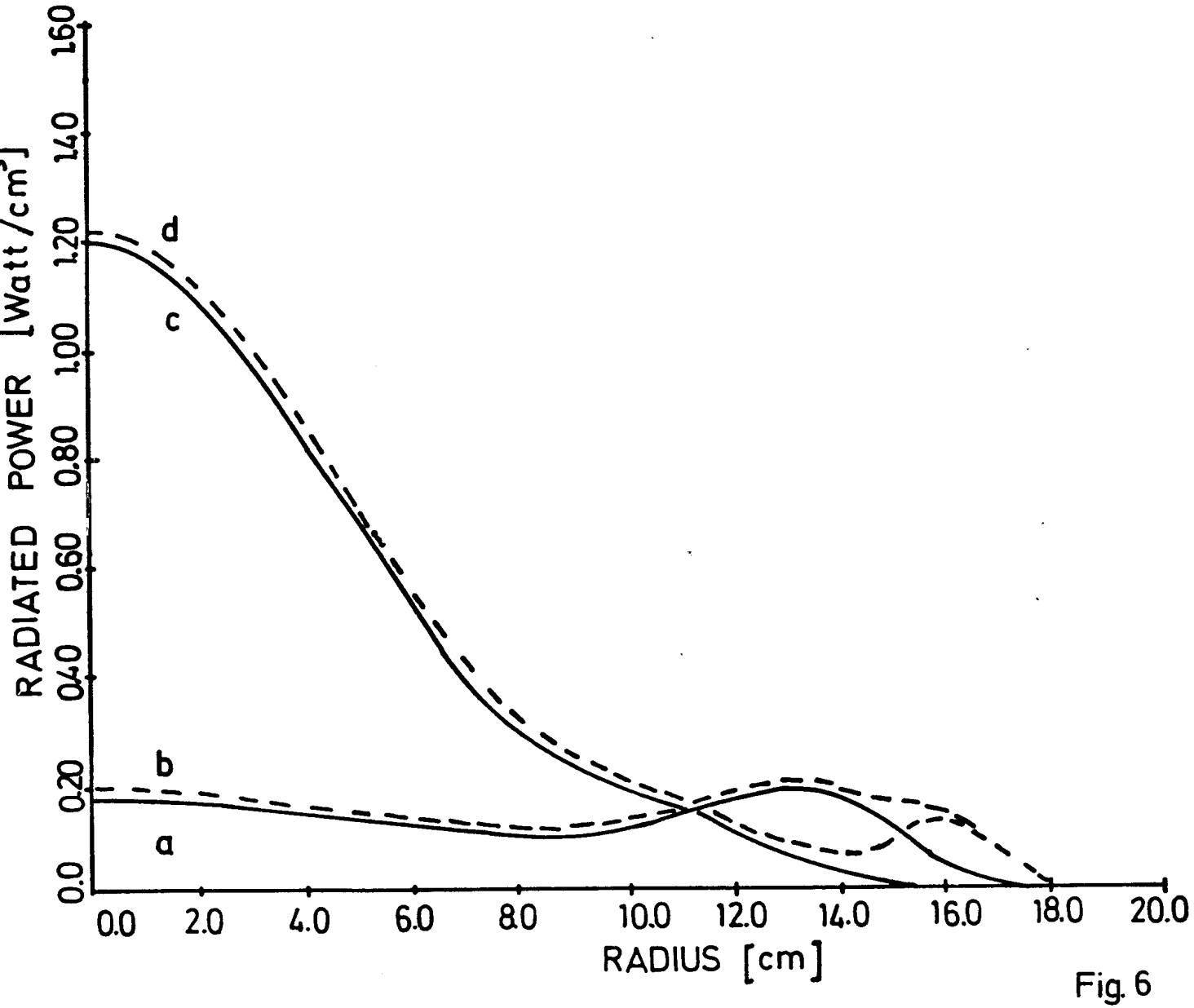
RADIATED POWER [Watt/cm²]
0.0
0.20
0.40
0.60
0.80
1.00
1.20
1.40
1.60
a
b
c
d
0.0
2.0
4.0
6.0
8.0
10.0
12.0
14.0
16.0
18.0
20.0
RADIUS [cm]

Fig. 6

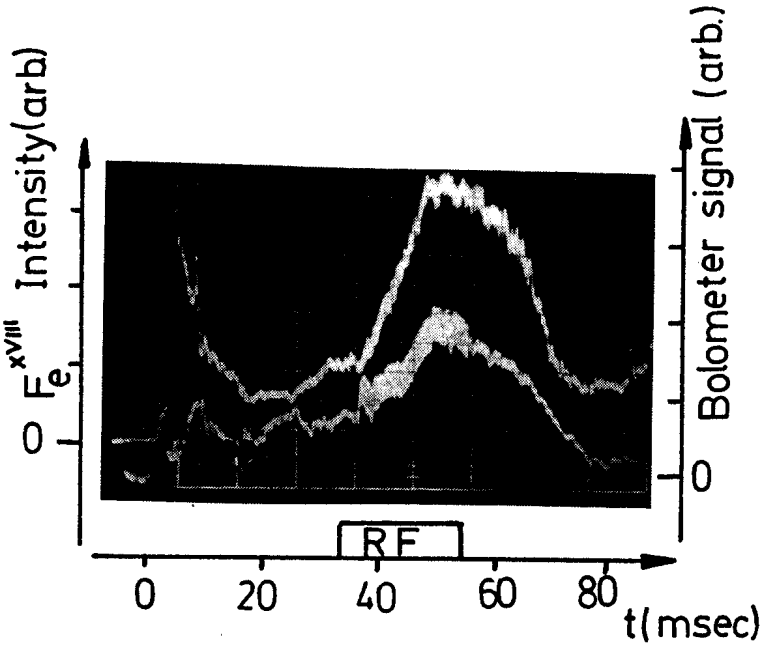
0 Fe^{XVIII} Intensity(arb)
Bolometer signal (arb.)
0
RF
0
20
40
60
80
t(msec)

Fig. 7

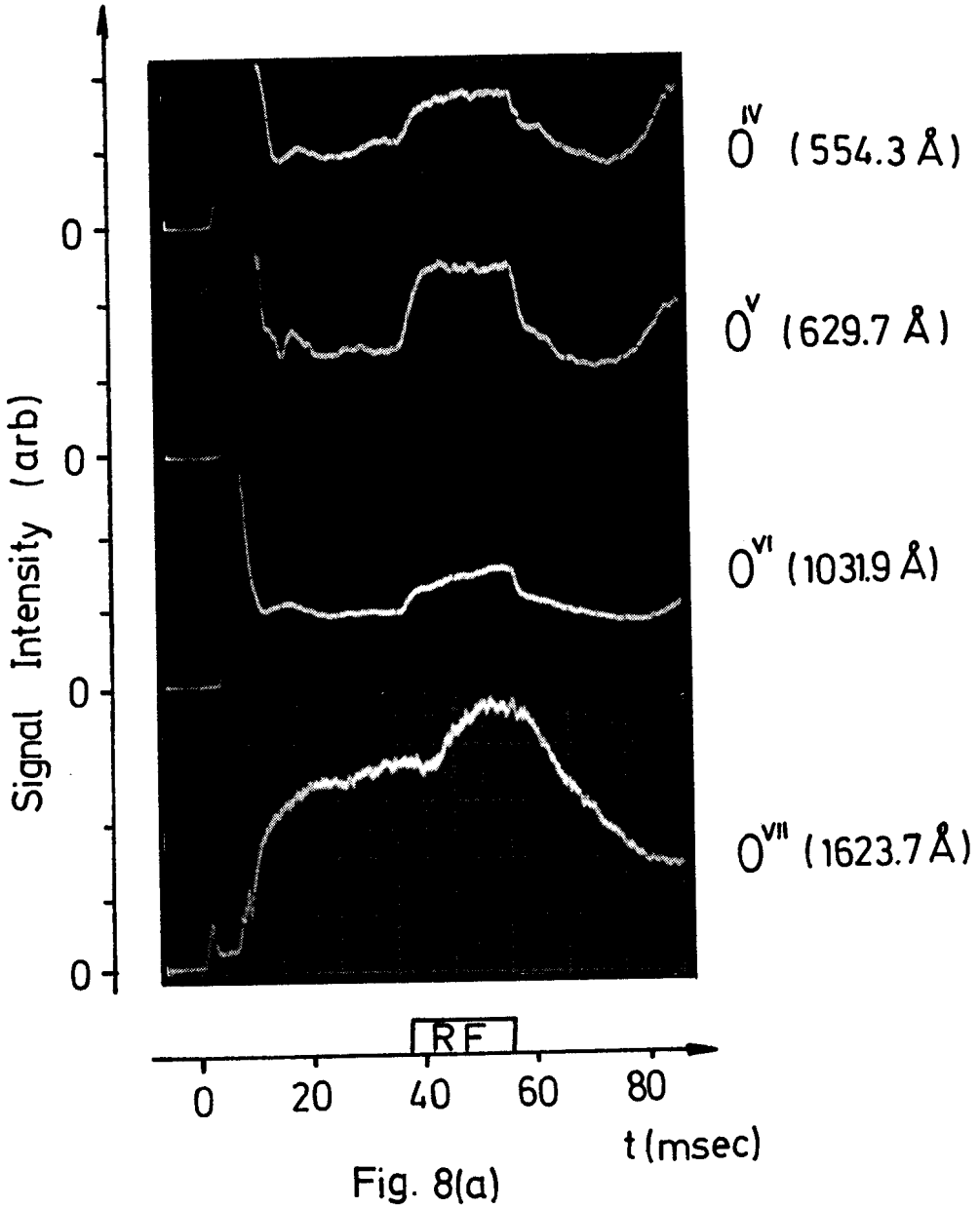
Signal Intensity (arb)
0
0
0
0
O^{IV} (554.3 Å)
O^{V} (629.7 Å)
O^{VI} (1031.9 Å)
O^{VII} (1623.7 Å)
RF
0
20
40
60
80
t (msec)

Fig. 8(a)

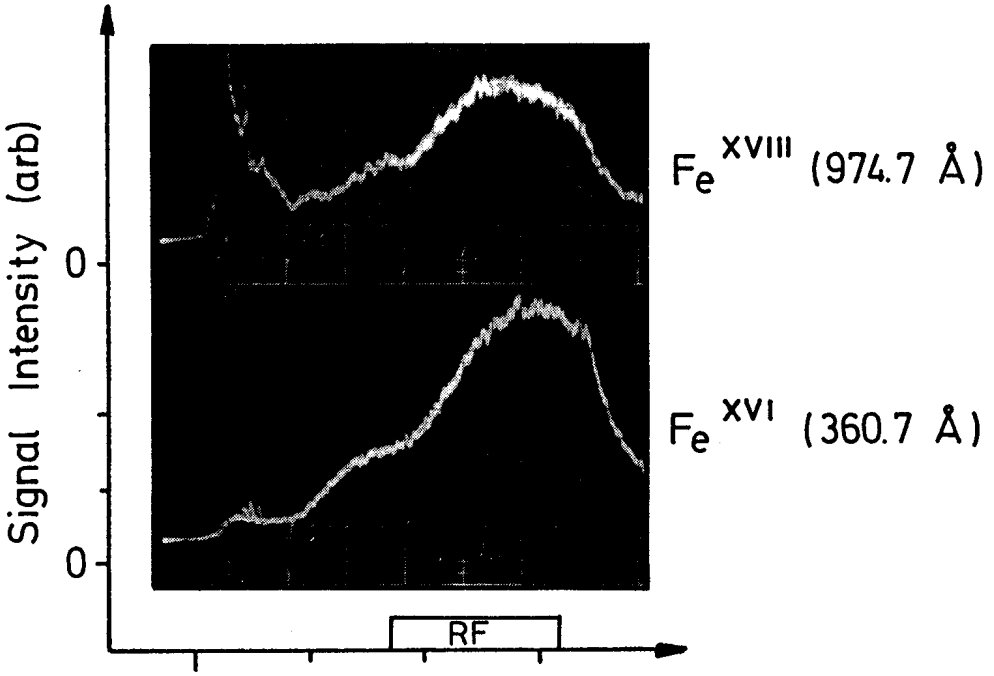
Signal Intensity (arb)
0
0
Fe^{XVIII} (974.7 Å)
Fe^{XVI} (360.7 Å)
RF
0
20
40
60
t (msec)

Fig. 8(b)

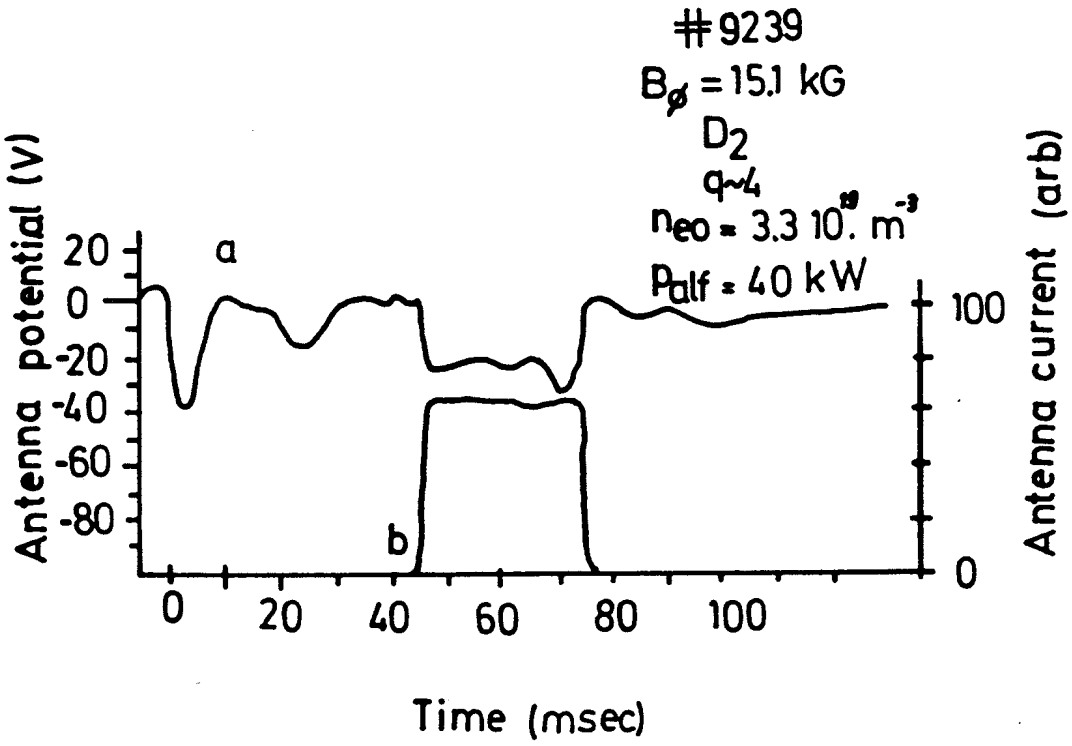
#9239
B_ϕ = 15.1 kG
D_2
q~4
n_{eo} = 3.3 10^{19} m^{-3}
P_{alf} = 40 kW
a
b
Antenna potential (V)
20
0
-20
-40
-60
-80
0
20
40
60
80
100
Time (msec)
100
0
Antenna current (arb)

Fig.9

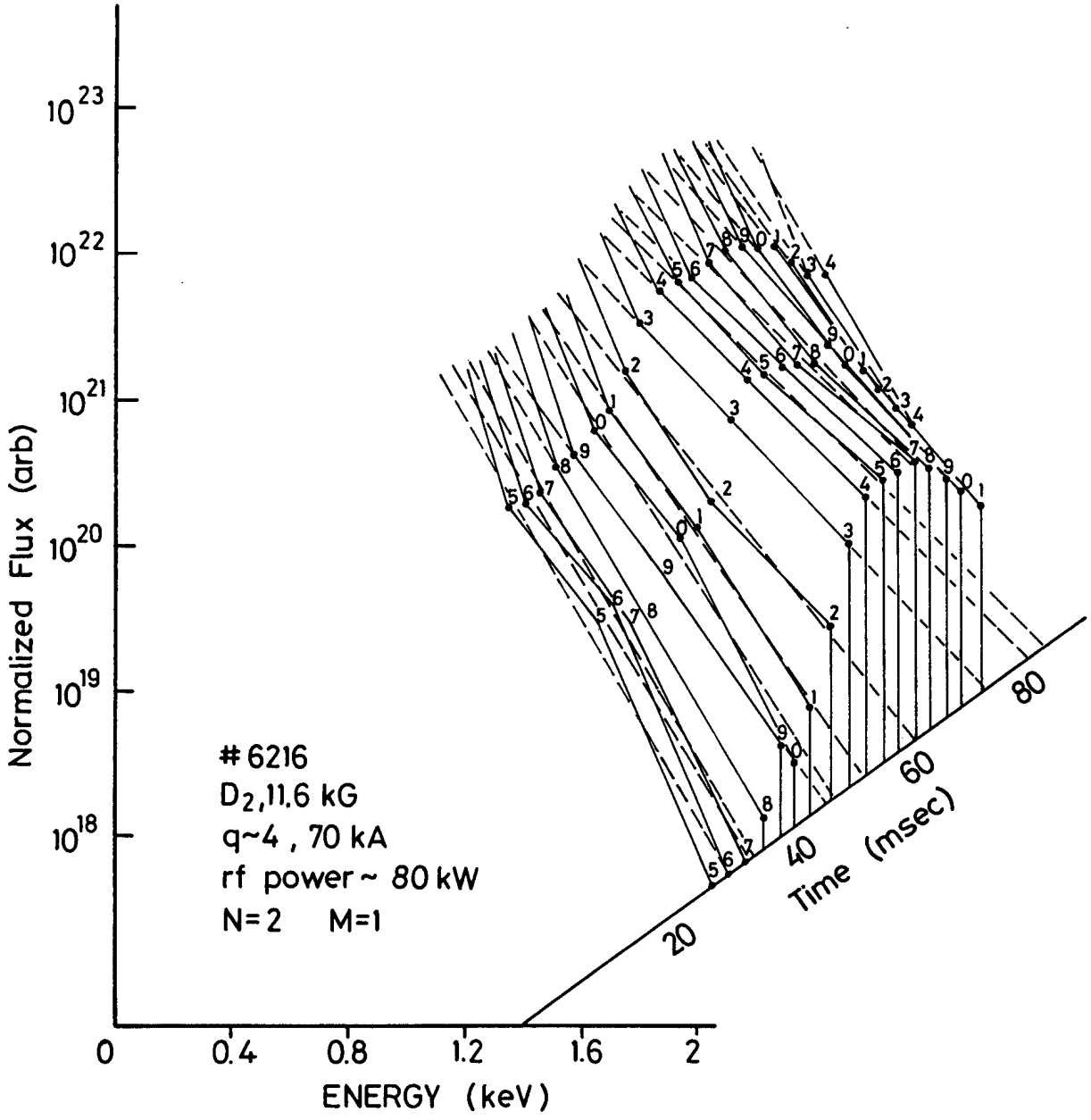
Normalized Flux (arb)
10^{23}
10^{22}
10^{21}
10^{20}
10^{19}
10^{18}
#6216
D_2, 11.6 kG
q~4 , 70 kA
rf power ~ 80 kW
N=2 M=1
0
0.4
0.8
1.2
1.6
2
ENERGY (keV)
20
40
60
80
Time (msec)

Fig. 10(a)

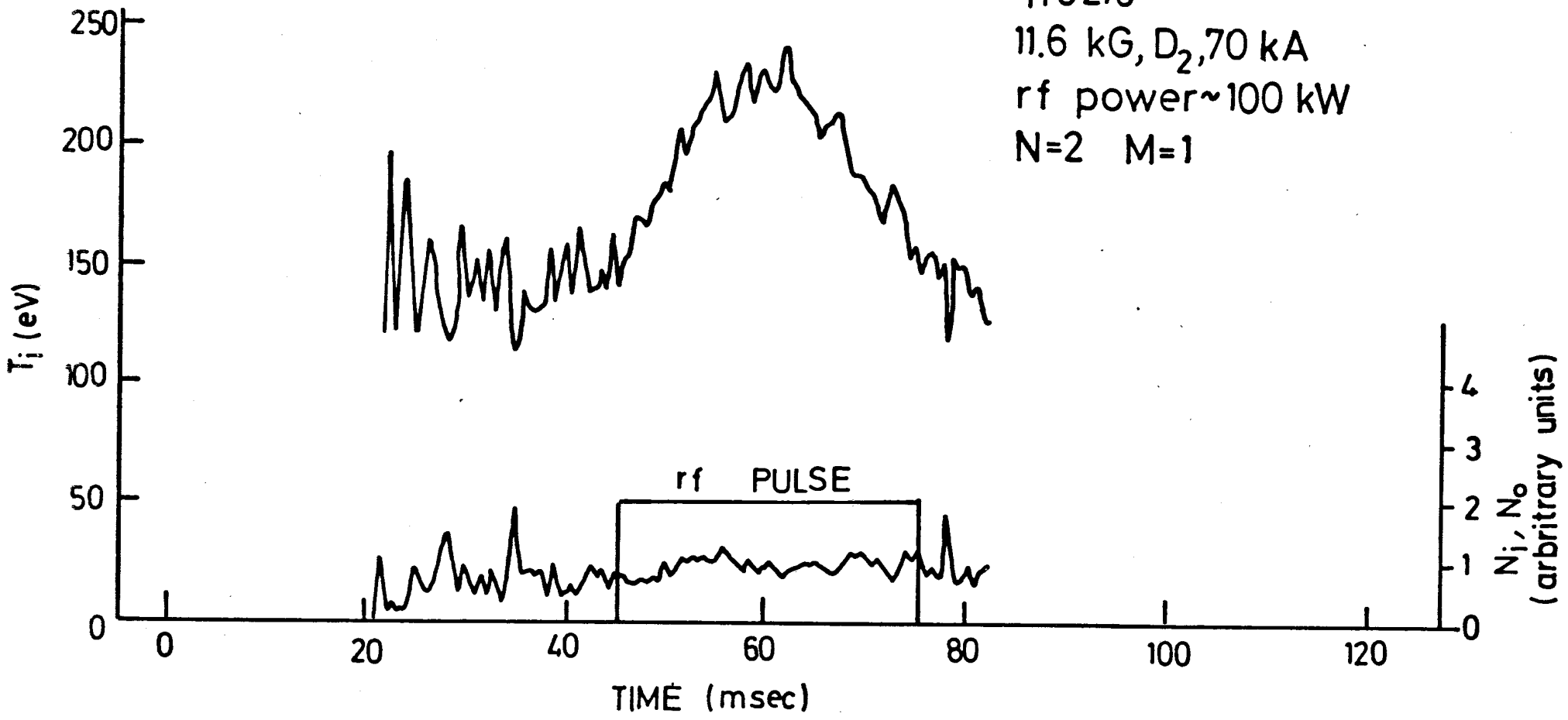
#6216
11.6 kG, D_2, 70 kA
rf power~100 kW
N=2 M=1
rf PULSE
T_i (eV)
N_i, N_o (arbitrary units)
TIME (msec)
0
50
100
150
200
250
0
20
40
60
80
100
120
1
2
3
4

Fig. 10(b)

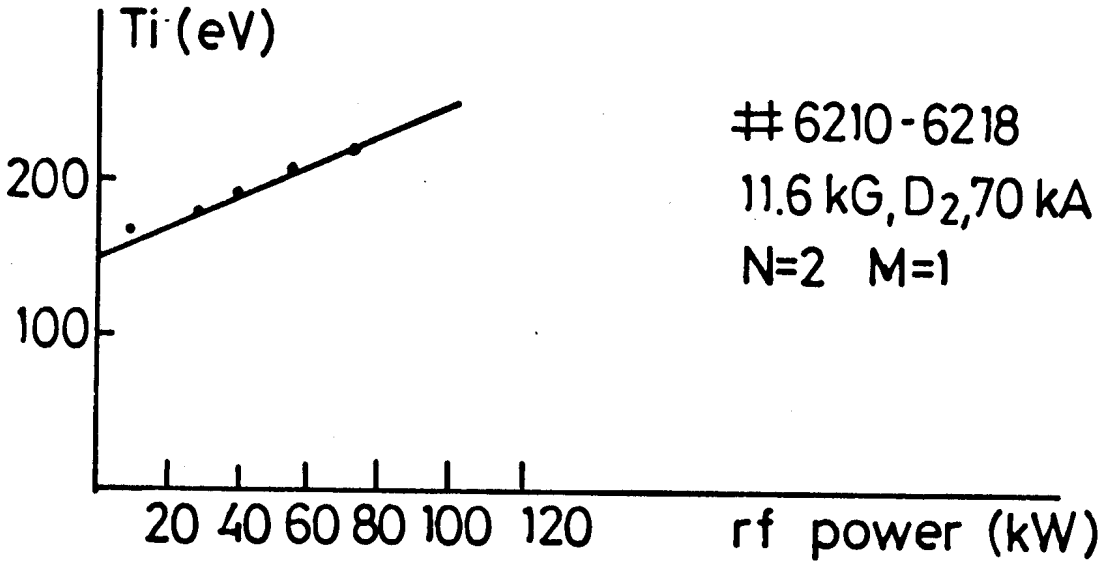
Ti (eV)
200
100
20 40 60 80 100 120
rf power (kW)
#6210-6218
11.6 kG, D2, 70 kA
N=2 M=1

Fig. 11

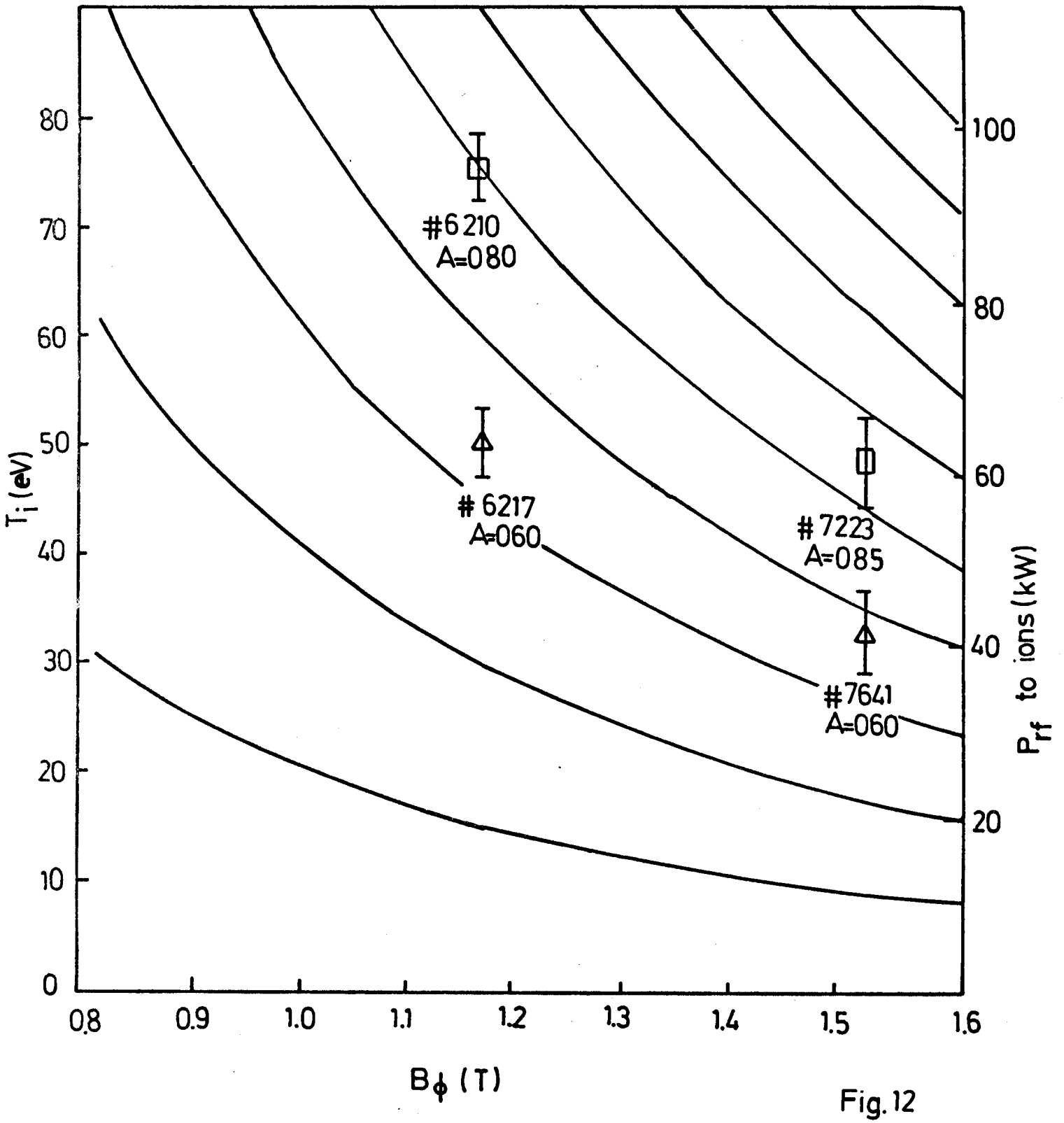
80
70
60
50
40
30
20
10
0
T_i (eV)
100
80
60
40
20
P_{rf} to ions (kW)
#6210
A=080
#6217
A=060
#7223
A=085
#7641
A=060
0.8
0.9
1.0
1.1
1.2
1.3
1.4
1.5
1.6
B_ϕ (T)

Fig. 12

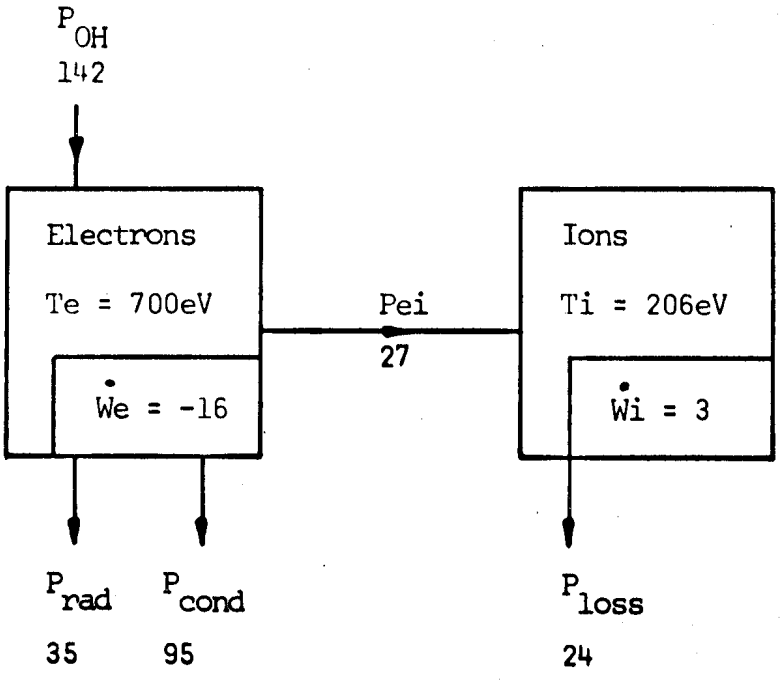

a)

(units = kW)

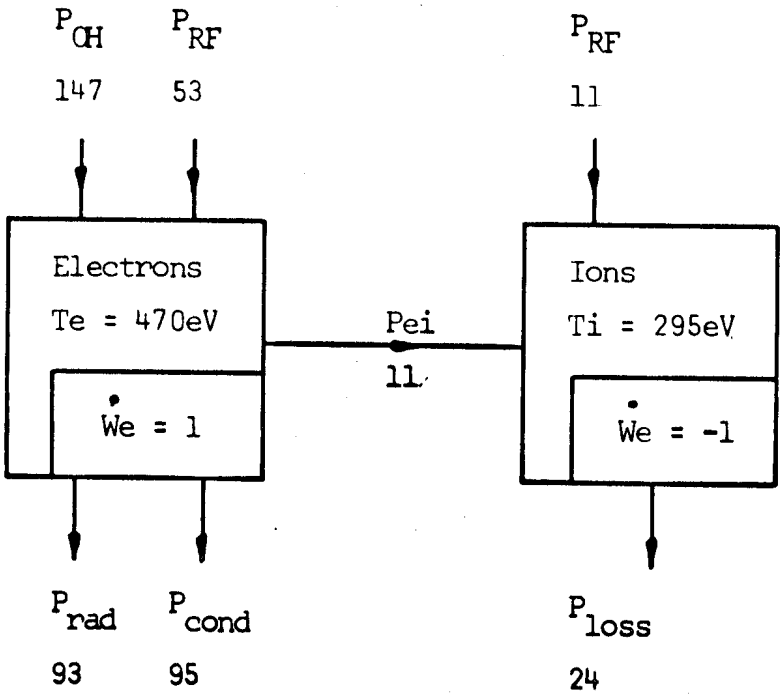

(units = kW)

b)

Fig. 13